Spin Hall magnetoresistance at the interface between platinum and cobalt ferrite thin films with large magnetic anisotropy

Takeshi Tainosho, Tomohiko Niizeki, Jun-ichiro Inoue, Sonia Sharmin, Eiji Kita, and Hideto Yanagihara

Citation: AIP Advances **7**, 055936 (2017); doi: 10.1063/1.4978582
View online: http://dx.doi.org/10.1063/1.4978582
View Table of Contents: http://aip.scitation.org/toc/adv/7/5
Published by the American Institute of Physics

Spin Hall magnetoresistance at the interface between platinum and cobalt ferrite thin films with large magnetic anisotropy

Takeshi Tainosho,[1] Tomohiko Niizeki,[2] Jun-ichiro Inoue,[1] Sonia Sharmin,[1] Eiji Kita,[1] and Hideto Yanagihara[1]
[1]*Division of Applied Physics, University of Tsukuba, Tsukuba 305-8573, Japan*
[2]*WPI-AIMR, Tohoku University, Sendai 980-8577, Japan*

(Presented 2 November 2016; received 23 September 2016; accepted 15 December 2016; published online 9 March 2017)

The recently discovered spin Hall magnetoresistance (SMR) effect is a useful means to obtain information on the magnetization process at the interface between a non-magnetic metal and ferromagnetic insulators. We report the SMR measurements at the interface between platinum and cobalt ferrite thin films for samples with two different preferential directions of magnetization (out-of-plane and in-plane). The directional difference of the magnetic easy axis does not seem to influence the value of SMR. [http://dx.doi.org/10.1063/1.4978582]

Spintronics is attracting many researchers from academia as well as industry.[1,2] In order to control the spin current, we have to develop techniques for the generation, transportation, and detection of the spin current. Among the many phenomena related to spintronics, the interface spin physics between magnetic and nonmagnetic materials is a field that is being actively researched. For example, spin pumping is a technique used to generate spin current through the dynamics of magnetization.[3,4] The spin Seebeck effect is a phenomenon used to convert thermal current to spin current.[5,6] Both phenomena originate from the spin Hall Effect (SHE) and can often be observed in a bilayer of non-magnetic metal (NM) and ferromagnetic metal (FM), and even in NM/ferromagnetic insulator (FMI) layers. SHE is a transport phenomenon used to convert the charge current to spin current through spin-orbit coupling, and the inverse effect (ISHE) is simply the opposite effect, which is useful for spin current detection.[7,8] Both the effects are expected to be larger in metals with a strong spin–orbit interaction such as Pt and Ta.[9]

A new type of magnetoresistance (MR) related to SHE was discovered in a Pt/YIG bilayer system and was named spin Hall magnetoresistance (SMR).[10,11] In the case of NM/FMI, which is a typical SMR system, the charge current flowing through the NM layer produces spin current via SHE, and the spins accumulate at the interface between the NM and FMI. Then, if the magnetization of FMI at the interface is parallel to the spins, the spin current will be reflected backwards. This backflow of spin current produces charge current via ISHE. On the other hand, the backflow will be suppressed if the magnetization of FMI is normal to the spin accumulation because part of the accumulated spins is transferred into the FMI layer through the interface. Therefore, the charge current via ISHE will decrease. The difference of these two conditions appears as a change of electrical conductance in the NM layer, depending on the magnetization orientations of the FMI layer. While the application of the conventional magnetometry technique to the hysteresis loops provides the magnetic signal of an entire sample, SMR can be a sensitive probe for interface magnetism.[12]

Many researchers have been studying SMR since its discovery.[13–16] Most of the experimental studies of SMR focus on a bilayer system with YIG as the FMI layer; YIG is one of the ideal FMI materials because it exhibits a very small magnetic anisotropy and has a significantly low damping factor. On the other hand, the physics of SMR in FMI with large magnetic anisotropy has not been investigated in detail; therefore, it is not clear how the magnetic anisotropy affects the transport of the spin angular momentum at the interface between NM/FMI.

Among many ferromagnetic oxides, cobalt ferrite (CFO) shows a significantly large magnetoelastic effect.[17,18] The easy axis can be varied between the out-of-plane and in-plane directions by changing the lattice distortion if CFO is in a film form. A previous report revealed that epitaxial CFO on MgO (001) shows a large perpendicular magnetic anisotropy of K_u of over 1 MJ/m^3 under a tensile strain.[19] Likewise, the in-plane magnetic anisotropy can be introduced by applying a compressive strain. The SMR at the interface between Pt and CFO has previously been investigated, but they did not focus on the magnetic anisotropy.[20,21] In this study, we report the SMR effect at the interface between Pt and $Co_{0.75}Fe_{2.25}O_4$ (CFO) (001) epitaxial thin films with two different preferential directions of magnetization (out-of-plane and in-plane) by controlling the magnetic anisotropy.

The CFO (001) thin films with two different preferential magnetic axes were grown on a MgO (001) substrate (a = 0.421 (2 a = 0.842) nm) and a $MgAl_2O_4$ (MAO) (001) substrate (a = 0.808 nm) by a reactive RF magnetron sputtering technique. We consider the lattice misfits depending on the substrates and conclude that the CFO (001) films grown on MgO (MAO) suffer from tensile (compressive) stress and exhibit a magnetically preferential axis parallel to the out-of-plane (in-plane) direction. Both the substrates were cleaned in ethanol and acetone by ultrasonic treatment for 5 min. After that, they were set into the sputtering chamber and heated to 773 K for 1 hour. A sputtering target of Fe-Co (Fe:Co = 3:1) alloy with a diameter of 2 inches was used. Ar and O were flowed as process gases. The flow rates (partial pressures) were 30 sccm (~0.5 Pa) and 6 sccm (~0.1 Pa) for Ar and O, respectively. The temperatures of the substrates were maintained at 773 K during the sputtering processes. The RF power was maintained at 100 W. After the CFO thin films were deposited, Pt Hall bars (length: l = 1000 μm, width: w = 300 μm, thickness: t = 7 nm) were fabricated on the CFO film with a metal mask by the DC sputtering technique at room temperature (RT). Ar was flowed at 30 sccm (~0.5 Pa) and the DC power was maintained at 20 W during the deposition.

The crystallinity and thickness of CFO thin films were evaluated by reflection high-energy electron diffraction (RHEED) and X-ray reflectivity. The MH-loops (-7 T < $\mu_0 H$ < 7 T) were measured by a magnetometer (Quantum Design, MPMS3) at RT. Angle dependent MR (ADMR, $\mu_0 H$ = 9 T) and field dependent MR (FDMR, -9 T < $\mu_0 H$ < 9 T) measurements were also performed at RT using the Physical Property Measurement System (Quantum Design).

The typical streak patterns of a spinel structure were observed by RHEED of CFO surfaces, which indicated the epitaxial growth of CFO thin films. The distance between the streaks of CFO films were almost half that of the MAO substrate despite the same crystal structure. This phenomenon was also observed while growing epitaxial Fe_3O_4 thin films on MgO (001) substrates.[22,23]

Figure 1 shows the MH-curves of CFO on MgO (001) and on MAO (001). Here, we supposed that the magnetization saturates over 6 T to subtract the background signal. The CFO film grown on MgO (MAO) exhibits perpendicular (in-plane) magnetic anisotropy, and the saturation magnetization is comparable to that of the bulk.

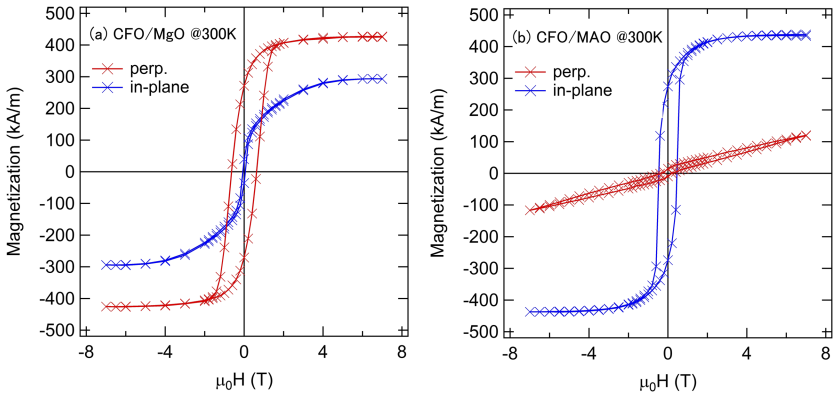

FIG. 1. MH-loops of (a) CFO/MgO and (b) CFO/MAO at 300K. Out-of-plane and in-plane magnetic anisotropy were confirmed for CFO/MgO and CFO/MAO.

The effective uniaxial magnetic anisotropy constant K_u evaluated by magneto-torque measurements at RT, was $K_u \sim 1$ MJ/m^3 and -5.2 MJ/m^3 for CFO/MgO and CFO/MAO, respectively.[17,24] Those values of K_u were extracted from the high-field torque data using Miyajima's analysis.[25] We note that the easy axis is defined as perpendicular to the film; therefore, a positive value of K_u means a perpendicular magnetization film.

The ADMR results are shown in Fig. 2. The SMR ratios for Pt/CFO/MgO (001) and Pt/CFO/MAO (001) are 0.074% and 0.073%, respectively. The charge current flows along the x-axis, and the films lie in the x-y plane in our configuration. The magnetic field ($\mu_0 H = 9$ T) was rotated in the x-y, y-z, and z-x plane, which are termed α-scan, β-scan, and γ-scan, respectively. The temperature was maintained at 300 K. According to the theory of SMR,[11] the longitudinal resistivity $\rho_{long} = R_L \cdot t \cdot w/l$ can be expressed as

$$\rho_{long} \approx \rho_0 + \rho_1 \left(1 - {m_y}^2\right), \tag{1}$$

where ρ_0 is a spin-independent term of the resistivity, ρ_1 indicates the component of SMR, R_L is the experimentally obtained longitudinal resistance, and $\mathbf{m} = (m_x, m_y, m_z)$ represents the direction cosine of the magnetization for each axis.

Since the estimated anisotropy field of CFO/MAO (001) is greater than 20 T, the SMR ratio in the β-scan (Fig. 2(e)) is possibly underestimated. One can see no apparent MR in γ-scans, where the geometry anisotropic magnetoresistance (AMR) can be observed in Fig. 2(c, f). This means that the MR observed in α- and β-scans should be explained by the SMR model rather than by AMR. The magnitude of the SMR is expressed by the following equation:[11]

$$\frac{\rho_1}{\rho_0} \approx \theta_s^2 \frac{\frac{2\lambda_{Pt}^2}{\sigma_{Pt} t_{Pt}} G_r tanh^2 \frac{t_{Pt}}{2\lambda_{Pt}}}{1 + \frac{\lambda_{Pt}}{\sigma_{Pt}} G_r coth \frac{t_{Pt}}{\lambda_{Pt}}}. \tag{2}$$

Here, θ_s, λ_{Pt}, t_{Pt}, σ_{Pt}, and G_r stand for the spin Hall angle, spin diffusion length, film thickness, Pt layer conductivity, and the real part of the spin mixing conductance at the interface, respectively.

Using plausible values of $\theta_s = 0.056$ and $\lambda_{Pt} = 3.4$nm for Pt, used in the previous research of which the conductivity of Pt layer is of the same order as our result ($2.8 \sim 3.2 \times 10^6$ ($\Omega^{-1} \cdot$m^{-1})),[26] the values of G_r are calculated to be 20.8×10^{14} $\Omega^{-1} \cdot$ m^{-2} and 21.1×10^{14} $\Omega^{-1} \cdot$ m^{-2} for Pt/CFO/MgO and Pt/CFO/MAO, respectively. These are an order of magnitude larger than the previously reported value for the Pt/CFO system if the estimation of θ_s and λ_{Pt} is appropriate.[20,27] Additionally, G_r could possibly be affected by the magnetic anisotropy energy strength and the preferential axis direction,

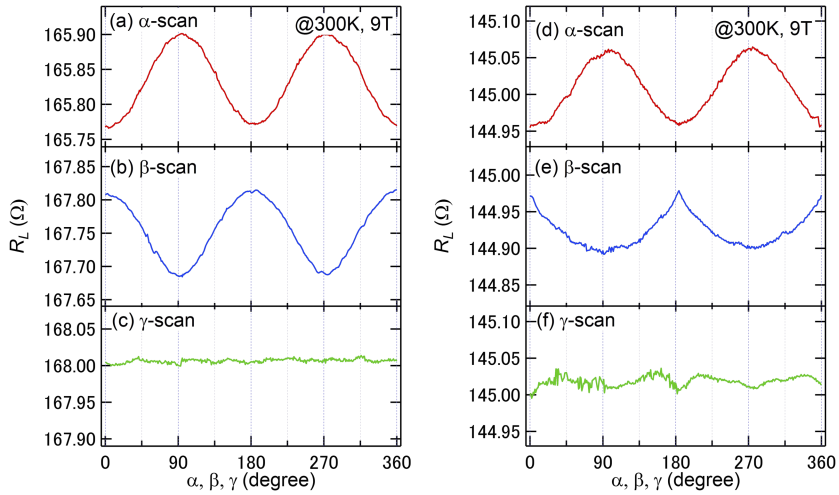

FIG. 2. Angle dependent MR (T = 300K, $\mu_0 H$ = 9 T) for Pt/CFO/MgO (a-c) and Pt/CFO/MAO (d-f). The schematic configuration is shown above, where the charge current flows along the x-axis and the longitudinal resistance R_L represents the resistance along the charge current direction. The typical angular dependence for SMR was confirmed for both samples.

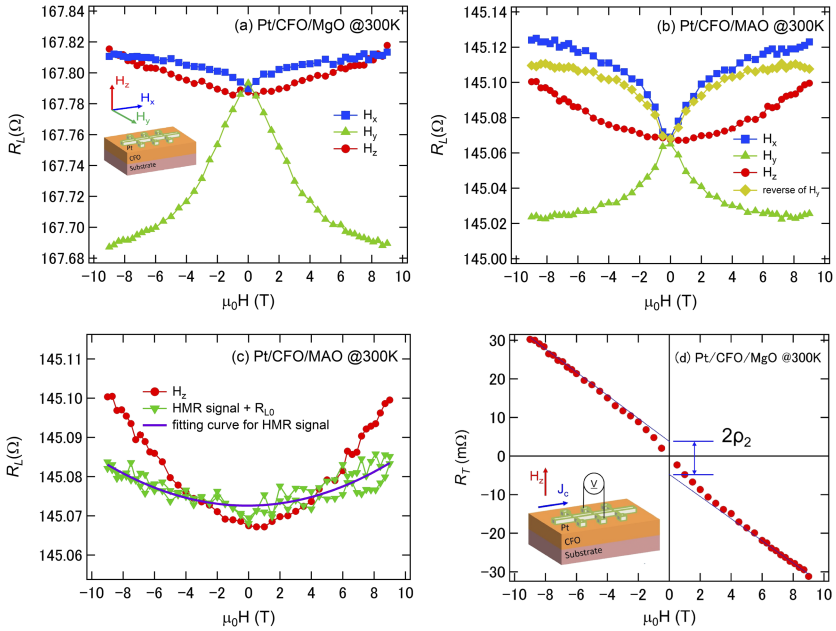

FIG. 3. Field dependent MR for Pt/CFO/MgO (a) and Pt/CFO/MAO (b) at 300K. The inset in Fig. 3(a) shows the magnetic field direction. The longitudinal resistance R_L represents the resistance along H_x. The Hanle MR signal was compared to R_L (H_z) curve of Pt/CFO/MAO as the base resistance R_{L0} is 145.068 Ω and parabolic purple line is the fitting curve for the HMR signal. In addition, an AHE-like signal was detected for Pt/CFO/MgO in the Hall geometry (d). The intercept of blue line at the vertical axis represents ρ_2 term (d).

because magnon gaps are dependent on those parameters. However, we cannot find any significant difference between the two highly anisotropic CFO samples with a different easy axis.

The field-dependent values of R_L for both samples are shown in Fig. 3. The variations in R_L for all three directions are qualitatively consistent with the magnetic anisotropy shown in the *MH*-loops. We note that R_L is dominated not only by SMR but also by the Hanle MR (HMR) arising from the dephasing of spin accumulation by the external field.[28] In the case of FDMR of Pt/CFO/MAO (001) shown in Fig. 3(b), one can see the asymmetry between R_L (H_x) and R_L (H_y). The inverted R_L (H_y) with respect to R_L (0) is plotted as a yellow curve. One can see the difference between R_L (H_x) and the inverted R_L (H_y). This difference can be attributed to the Hanle effect and the estimated MR ratio is 7×10^{-5} between $\mu_0 H = 0$ and 9 T. In Fig. 3(c), R_L (H_z) and the difference of R_L (H_x) and the inverted R_L (H_y) are plotted. The resistance corresponding to HMR exhibits less variation than the R_L (H_z) curve, suggesting that R_L (H_z) was determined by not only HMR but also SMR. In the case of Pt/CFO/MgO (001) shown in Fig. 3(a), both R_L (H_x) and R_L (H_z) exhibit positive MR even in the high field region, which mainly originates from HMR.

Finally, we would like to discuss the imaginary part of the spin-mixing conductance G_i. The transverse resistivity of Pt/CFO/MgO was obtained under Hall geometry. The non-zero value of the transverse resistivity at zero field can be seen in Fig. 3(d), which is similar to the coexistence situation of the anomalous Hall effect (AHE) on the ordinary Hall effect. The transverse resistivity driven by the AHE-like phenomenon is expressed as

$$\rho_{trans}^{SHAHE} \approx -\rho_2 m_z. \tag{3}$$

ρ_2 is the contribution of the imaginary part of the spin mixing conductance G_i[11] and corresponds to the intercept of the blue line at the vertical axis in Fig. 3(d). The estimated G_i is $3.9 \pm 0.3 \times 10^{14}$ $\Omega^{-1} \cdot m^{-2}$. Therefore, the ratio of $G_i/G_r = 0.19$, which is larger than the values in the previous studies of Pt/YIG.[13,14]

In summary, we showed the SMR at the interface between Pt and CFO (001) thin films with two types of magnetic anisotropy (out-of-plane and in-plane). The *MH*-loop of CFO/MgO (001) indicated that the preferential axis is out-of-plane while that of CFO/MAO (001) is in-plane. The SMR ratios

of these samples are nearly the same, meaning that the strong anisotropy does not directly affect the SMR. The FDMR of Pt/CFO on MgO and MAO indicated that HMR appears as a comparable contribution to SMR. In this way, our results suggest that the SMR can be a probe to detect the magnetic anisotropy at the surface of FMI. G_i was approximately ten times smaller than G_r, and this indicated that the perpendicular magnetic anisotropy does not have any notable influence on G_i.

ACKNOWLEDGMENTS

This work was supported by JSPS KAKENHI Grant Numbers JP15H03966 and JP15K13355.

[1] J. Sinova and I. Žutić, Nat. Mater **11**, 368 (2012).
[2] F. J. Jedema, A. T. Filip, and B. J. van Wees, Nature **410**, 345 (2001).
[3] Y. Tserkovnyak, A. Brataas, and G. E. W. Bauer, Phys. Rev. B **66**, 224403 (2002).
[4] S. K. Watson, R. M. Potok, C. M. Marcus, and V. Umansky, Phys. Rev. Lett. **91**, 250301 (2003).
[5] K. Uchida, S. Takahashi, K. Harii, J. Ieda, W. Koshibae, K. Ando, S. Maekawa, and E. Saitoh, Nature **455**, 778 (2008).
[6] J. Xiao, G. E. W. Bauer, K. Uchida, E. Saitoh, and S. Maekawa, Phys. Rev. B **81**, 214418 (2010).
[7] J. E. Hirsch, Phys. Rev. Lett. **83**, 1834 (1999).
[8] E. Saitoh, M. Ueda, H. Miyajima, and G. Tatara, Appl. Phys. Lett. **88**, 182509 (2006).
[9] H. Kontani, T. Tanaka, D. S. Hirashima, K. Yamada, and J. Inoue, Phys. Rev. Lett. **102**, 016601 (2009).
[10] H. Nakayama, M. Althammer, Y. T. Chen, K. Uchida, Y. Kajiwara, D. Kikuchi, T. Ohtani, S. Geprags, M. Opel, S. Takahashi, R. Gross, G. E. W. Bauer, S. T. B. Goennenwein, and E. Saitoh, Phys. Rev. Lett. **110**, 206601 (2013).
[11] Y. T. Chen, S. Takahashi, H. Nakayama, M. Althammer, S. T. B. Goennenwein, E. Saitoh, and G. E. W. Bauer, Phys. Rev. B **87**, 144411 (2013).
[12] M. Isasa, S. Vélez, E. Sagasta, A. Bedoya-pinto, N. Dix, F. Sánchez, L. E. Hueso, J. Fontcuberta, and F. Casanova, Phys. Rev. Appl. **6**, 034007 (2016).
[13] M. Althammer, S. Meyer, H. Nakayama, M. Schreier, S. Altmannshofer, M. Weiler, H. Huebl, S. Geprags, M. Opel, R. Gross, D. Meier, C. Klewe, T. Kusche, J. M. Schmalhorst, G. Reiss, L. Shen, A. Gupta, Y. T. Chen, G. E. W. Bauer, E. Saitoh, and S. T. B. Goennenwein, Phys. Rev. B **87**, 224401 (2013).
[14] N. Vlietstra, J. Shan, V. Castel, B. J. van Wees, and J. Ben Youssef, Phys. Rev. B **87**, 184421 (2013).
[15] Z. Ding, B. L. Chen, J. H. Liang, J. Zhu, J. X. Li, and Y. Z. Wu, Phys. Rev. B **90**, 134424 (2014).
[16] C. Hahn, G. de Loubens, O. Klein, M. Viret, V. V. Naletov, and J. Ben Youssef, Phys. Rev. B **87**, 174417 (2013).
[17] T. Niizeki, Y. Utsumi, R. Aoyama, H. Yanagihara, J. Inoue, Y. Yamasaki, H. Nakao, K. Koike, and E. Kita, Appl. Phys. Lett. **103**, 162407 (2013).
[18] G. Hu, J. H. Choi, C. B. Eom, V. G. Harris, and Y. Suzuki, Phys. Rev. B **62**, 779 (2000).
[19] H. Yanagihara, Y. Utsumi, T. Niizeki, J. Inoue, and E. Kita, J. Appl. Phys. **115**, 17A719 (2014).
[20] M. Isasa, A. Bedoya-Pinto, F. G. Saül Vélez, F. Sánchez, L. E. Hueso, J. Fontcuberta, and F. Casanova, Appl. Phys. Lett. **105**, 142402 (2014).
[21] H. Wu, Q. Zhang, C. Wan, S. S. Ali, Z. Yuan, L. You, J. Wang, Y. Choi, and X. Han, IEEE Trans. Magn. **51**, 4100104 (2015).
[22] S. A. Chambers and S. A. Joyce, Surf. Sci. **420**, 111 (1999).
[23] A. Subagyo and K. Sueoka, Jpn. J. Appl. Phys. **45**, 2255 (2006).
[24] T. Tainosho, J. Inoue, S. Sharmin, E. Kita, and Y. Hideto (unpublished).
[25] H. Miyajima, K. Sato, and T. Mizoguchi, J. Appl. Phys. **47**, 4669 (1976).
[26] J.-C. Rojas-Sanchez, N. Reyren, P. Laczkowski, W. Savero, J. Attané, C. Deranlot, M. Jamet, J. George, L. Vila, and H. Jaffrès, Phys. Rev. Lett. **112**, 106602 (2014).
[27] E. Sagasta, Y. Omori, M. Isasa, M. Gradhand, L. E. Hueso, Y. Niimi, and Y. Otani, Phys. Rev. B **94**, 060412 (2016).
[28] S. Vélez, V. N. Golovach, A. Bedoya-pinto, M. Isasa, E. Sagasta, M. Abadia, C. Rogero, L. E. Hueso, F. S. Bergeret, and F. Casanova, Phys. Rev. Lett. **116**, 016603 (2016).